PERIODICA POLYTECHNICA SER. MECH. ENG. VOL. 45, NO. 2, PP. 135–155 (2001)

FE ANALYSIS OF THE CONTROL METHODS USED IN CRIMPING OF JOINTS WITH POLYMER COMPOSITE CORES

Oleg I. BENEVOLENSKI and György KRÁLLICS

Department of Materials Science and Engineering
Budapest University of Technology and Economics
H – 1521 Budapest, Hungary

Received: Dec. 5, 1999

Abstract

This paper presents results of the Finite Element analysis of crimped cylindrical joints with polymer composite cores. Initial data of the Finite Element analysis significantly affecting results of the simulation are design parameters and mechanical properties of the components. Initial interface clearance of the joint and hardening behaviour of the steel sleeve were found to have special importance. Material testing, and dimension analysis are conducted to find the parameters' variation limits. Performed Finite Element parametric study allowed to compare quality of existing technological parameters in respect to residual strain energy of the core chosen as a measure of the load-bearing capacity. Analysis showed that extra mechanical work parameter is the most robust to variation of dimensions and mechanical properties.

Keywords: cylindrical joint, composite core, residual strain energy, extra mechanical work.

1. Introduction

Modern Fibre Reinforced polymer (FRP) composites demonstrate a number of advantages compared to conventional materials. These are high specific stiffness and strength, flexibility, chemical resistance, etc. Incorporation of composite parts into the structures of critical mechanical performance necessitated development of individual fastening techniques with metallic and other non-composite counterparts.

Heavily loaded cylindrical joint with fibre reinforced composite is widely applied recently producing end-fittings of non-ceramic electrical insulators [1], [5] and fittings of composite transmission shafts and pipes. Rough sketch of the joint is depicted in *Fig. 1*. Cylindrical joint consists of load-bearing composite core *1* firmly affixed in metal sleeve *2*. The mean of the load resistance is cylindrical interface between core and sleeve. It may be provided by contact pressure or adhesive bonding. Assembled joints are subjected to tensile or compressive axial force F, torsion T and bending moment M during the service. Composite core may be exposed to nearly critical loading in the course of both assembling and the lifetime. This may result in brittle fracture of the core. On the other hand, axial, bending or torsion service loads will dismount too weak joint. Such kind of joint's failure may be extremely hazardous in the most of applications as in the case of High Voltage overhead electrical insulation and automotive practice.

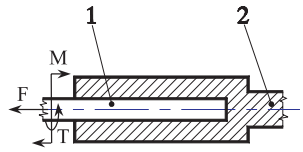

Fig. 1. Scheme of a tight cylindrical joint

Due to a number of practical considerations (such as reliability, low cost, and reproducibility) compression type joints become recently state-of-the-art in composite insulators technology [5]. Patent search [6] also showed, that assembling of end-fittings of composite electrical insulators is represented nowadays by inward crimping, or squeezing, of metal cylindrical fitting in dies of radial motion (*Fig. 2*).

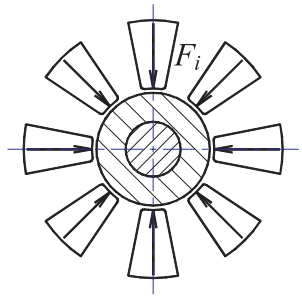

Fig. 2. Crimping of cylindrical joint in dies of radial motion

Crimping is a cold metal forming process involved to develop residual plastic deformations in the metal sleeve. Necessity of contact pressure existence in the interface assumes transversal loading of composite core, which reaches its extreme at the maximum of applied load, then relaxing partly after unloading. When joint is unloaded residual plastic strains remain in the fitting, while core tends to spring back elastically. It causes residual radial elastic stresses in both components and contact pressure upon the interface.

Degree of forming may be most easily quantitatively characterised by applied forming force and/or effective displacement of the tool. Therefore working load and tool's position are known as traditionally applied technological parameters. These parameters are sensitive to variation of dimensions and/or mechanical properties of the metal sleeve. It means that crimping until certain value of load or displacement may produce unacceptable variation of load-bearing capacity of assembled joints due to variation of initial contact clearance or steel sleeve thermal treatment conditions. An alternative control method, having well defined physical meaning and based on the estimation of extra mechanical work was proposed recently by BENEVOLENSKI–TÉGLÁS [4].

In this paper the authors analysed the factors affecting assembling process

and joints performance. Detailed materials testing study is performed to specify properties' scattering band. Finite Element study is conducted to compare available control methods and their robustness to variation of dimension and mechanical properties.

2. Analysis of the Factors Influencing Crimping Process

Load-bearing capacity of joints in assumption of pure mechanical interface is primarily controlled by distribution and magnitude of the contact pressure in the interface [2]. If former is mainly affected by design factors and tools geometry then later can be completely altered during the crimping. Residual pressure in the interface is reflection of the compression state achieved, which can be integrally accessed through the residual strain energy of the compressed core. Two most easily accessible process variables extensively used by designers and engineers for characterising and control of the crimping process are forming load and position of the tool. Traditionally each of them was treated separately in corresponding one-dimensional space as threshold or limiting value. Summarising existing control methods let authors schematically represent crimping process by linear piece-wise curve in 2-dimensional load-position co-ordinate system (*Fig. 3*).

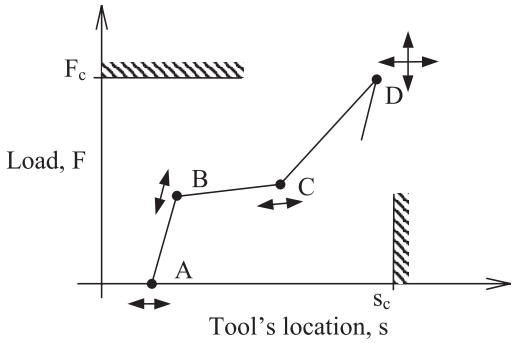

Fig. 3. Existing control parameters in the load-position space

Segment *AB* represents monotonous loading of the sleeve accompanied by small deformations mainly in elastic region. It is followed by segment *BC* corresponding to the plastic yielding in the bulk of the sleeve. Departure in point *C* associated with sudden increase in stiffness is attributed to the contact with the core and change in contact and boundary conditions of the system. Maximum load and displacement is achieved in point *D*, after which unloading follows.

Relative location of point *A* is essentially affected by initial external diameter of the sleeve. For bigger sleeves contact will happen earlier (point *A* moves to the left) and smaller sleeve will shift it to the right. Slope *AB* is dependent on the sleeve's elasticity modulus and design parameters (contact conditions, effective

length and so on). With other factors constrained height of point B is mainly a function of yielding stress of the sleeve material. For given design slope BC is primarily affected by the work hardening rate of the sleeve material. Length BC is mainly a function of initial clearance in the interface. The bigger is the clearance the longer BC lasts. Absolute abscissa of point C, however, is defined by both initial external diameter of sleeve and clearance in the interface. Both stiffness and compressibility of composite rod and formability of the sleeve affect slope CD, where final position (point D) is a *function of all mentioned factors and a subject to variation in both x and y directions.*

Two traditional control methods–by force and position–are depicted by F_c and s_c constraints correspondingly. Alteration of factors influencing location of point D would make probably both of the control parameters ineffective. One can intuitively guess, however, that some other parameter (as length CD for instance) would represent actual compression degree of composite core much better invariantly to its absolute location in $F - s$ space.

Presented theoretical reasoning allows announcing two main phenomena affecting particular shape of the load diagram and, hence, compression degree of the core. These are material properties and dimensions of the components. If by any reason variation of each of them is high enough problems of controllability of the process appear. Practice shows that such variation is inevitable.

2.1. Analysis of Dimensions and Tolerances

One of the most critical dimension factors influencing crimping and, hence, load-bearing capacity is initial clearance of the joint m. Later, analysis will handle mainly this value understanding, however, that presented considerations are valid for the external diameter of the sleeve as well.

JUVINALL et al. [7] classifies fits with least (guaranteed) clearance ($l > 0$) in decreasing order as loose, free and medium correspondingly and as snug fit for $l = 0$. Habitually, joints prior to crimping are designed to be designated as medium fits (*Fig. 4*). Actual clearance m is constrained by the relation

$$m_{\min} \le m \le m_{\max} \Leftarrow m_{\min} = l \qquad \text{and} \qquad m_{\max} = l + t_c + t_s. \tag{1}$$

Variation of m thus may be specified in the band

$$m_{\max} - m_{\min} = t_c + t_s, \tag{2}$$

where t_c – tolerance zone of the core, and t_s – tolerance zone of the sleeve correspondingly. According to the data from the manufacturers, bore has normally as turn finishing which for diameter d in the range 15–20 mm provides tolerance band equal to 0.10 mm. Pultruded composite rod has usually higher precision and may guarantee tolerance band of 0.05 mm. *Eq.* (2) yields value of 0.15 mm. Value 0.20 mm is chosen as a base for clearance variation in the Finite Element (FE) simulation.

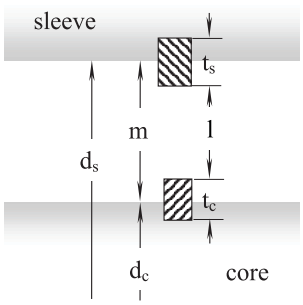

Fig. 4. Tolerance zones' distribution in loose, free or medium joints

2.2. Analysis of Material Properties of Sleeve

Selection of materials used for metal sleeve production is mainly governed by following criteria: formability, sufficient mechanical performance and low cost. Satisfaction of these requirements usually results in selection of carbon steel or casting iron with the carbon contents of at least 0.10–0.20%. For some components inferior mechanical characteristics are restricted by standardised dimensions (critical cross-section) of mating attachments. Thus material may be assigned, for instance, to have tensile strength of at least 350 MPa. Examples of such steels are MSZT Fe235B, DIN C15, C40 and many others.

LAHTIN [14] indicated that mechanical properties of normal quality carbon steel (e.g. MSZT Fe235B or GOST St3) used for production of many structural components may demonstrate large scattering of main mechanical characteristics due to the variation of chemical composition and difference in thermo-mechanical history. Thus, yielding stress may be increased in 1.5 times, and strength up to 2 times. Restriction of requirements to the chemical composition (utilisation of higher quality steel) or thermo-mechanical treatment (annealing with cooling in oven) enlarges cost of raw material and total production cost. The worth may totally rise by up to 50%.

At any reasonable choice of material, mechanical characteristics of the component would vary from piece to piece and from lot to lot. Testing of the metal sleeves arrived from a subcontractor prior to assembling is possible by producing tensile or upsetting specimens from the bulk of a sleeve, thus destroying the component. Satisfactory result does not necessarily mean that next workpiece from the lot will be identical. Production of test specimens is time and cost consuming. Non-destructive methods like local hardness measurement do not always prove good correlation with bulk mechanical characteristics.

Provided considerations show, that natural and inevitable scattering of mechanical characteristics of the steel component may result in variation of the core's compression degree while crimping for the same forming load. Restriction of the chemical composition or thermo-mechanical treatment may essentially raise the

cost, while the main problem remains unaffected. Conducted material testing study, described below, is aimed to estimate the scattering of mechanical characteristics typical for materials used in production of metal sleeves.

2.2.1. Continuous Upsetting of Specimens with Angular Groves

Results of simple tensile test on specimens produced from the fittings of electrical composite insulators were reported in [3]. Basic material was MSZT Fe235B. Prior to testing, parts undergo following sequence of thermo-mechanical transformations: hot rolling → forging → annealing. The results basically coincided with those in [14]. Continuous upsetting performed on the same specimens is described below.

Upper and bottom cavities of specimens with angular groves were filled with molybdenum sulphide – high-pressure lubricant – to produce almost frictionless (hydrodynamic friction with friction coefficient of two orders of magnitude smaller) upsetting conditions. This eliminated barrelling and guaranteed uniformity of stress distribution. Finally it resulted in beneficial conditions for uniaxial compression in a large deformation range. This method is considered [13] to be one of the most exact in definition of true hardening behaviour in compression.

Assumption of the volume conservation under plastic deformation yielding from the incompressibility condition maintains the relation between axial displacement and change in the cross-section area:

$$V = A_0 \cdot h_0 = A \cdot h, \tag{3}$$

where V is the volume of the specimen, A_0 and A are initial and actual cross-section area, and h_0 and h are initial and actual height of the specimen. Then, true stress may be calculated

$$\sigma = \frac{F}{A} = \frac{F}{A_0} \cdot \frac{h}{h_0}. \tag{4}$$

Corresponding true (logarithmic) plastic strain (neglecting elastic component) is calculated as

$$\varepsilon_{pl} = \ln \frac{h_0}{h}. \tag{5}$$

Results of the measurement are plotted in *Fig 5*.

2.2.2. Analysis of Materials Test Results and Assignment of Properties Variation

KROHA [13] analysed true stress–strain diagrams of many carbon steels. He showed that they are well approximated by the power function

$$\sigma = m\varepsilon_{pl}^{n} \tag{6}$$

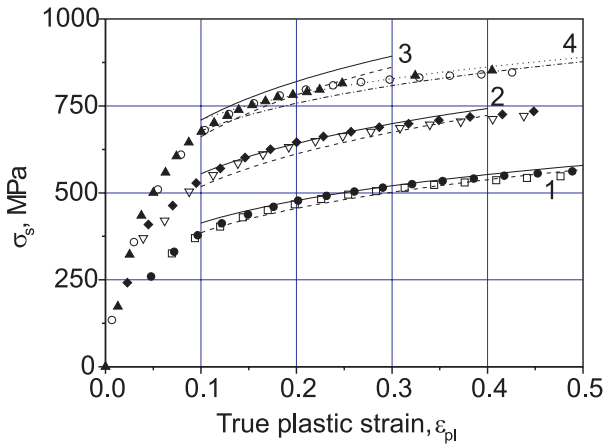

Fig. 5. Upsetting of carbon steel Fe 235B MSZT: dots, test results; lines, analytical hardening curves $\sigma = m\varepsilon_{pl}^{n}$: $1-m = 670$ MPa; $2-m = 900$ MPa; $3-m = 1150$ MPa; solid lines, $n = 0.21$; dash lines, $n = 0.24$; $4-m = 980$ MPa; dot line, $n = 0.14$; dash-dot line, $n = 0.16$

for the range of plastic strains $\varepsilon_{pl} = 0.1-1.0$. Parameter n is called work hardening rate and defines the ability of material to strain hardening with progressing plastic deformations. By taking natural logarithm of the left and right sides of *Eq.* (6) parameters n and $\ln(m)$ may be found exactly by means of linear fitting. Authors, however, kept the same reference frame $(\sigma - \varepsilon_{pl})$, since they intended to show the zone of possible mechanical characteristic variation rather than to exactly fit particular datasheet.

According to [9] hardening rate of the studied carbon steel lies in the range 0.215 and 0.23. Empirical relation by PYSZ [10] transformed to MPa-mm unit system has form:

$$m \approx 1.83 s_{\max} + 39.2. \tag{7}$$

This steel is known to resist guaranteed tensile strength at least $s_{\max} \approx 350$ MPa. *Eq.* (7) yields $m_{\min} \approx 670$ MPa. Analytical curves 1, 2 and 3 of *Fig. 6* are constructed for $m > 670$ and $n = 0.21 - 0.24$. Curve 4 appears to better match higher yielding stress data. It reduces n to $0.14 - 0.16$.

For quality carbon steel gathering of mechanical characteristics is somewhat better. The influence of chemical content is minimised and hardening rate is rather altered by the thermal treatment. Different literature sources may also show alteration of mechanical properties. Aside from mentioned previously these differences are explained by measurement errors and differences in testing conditions (testing procedure, deformation rate, and temperature effect). Comparison of work hardening characteristics for carbon steel C15 DIN from different sources is provided in *Fig. 6.* Thick lines are constructed to approximately cover the range of mechanical

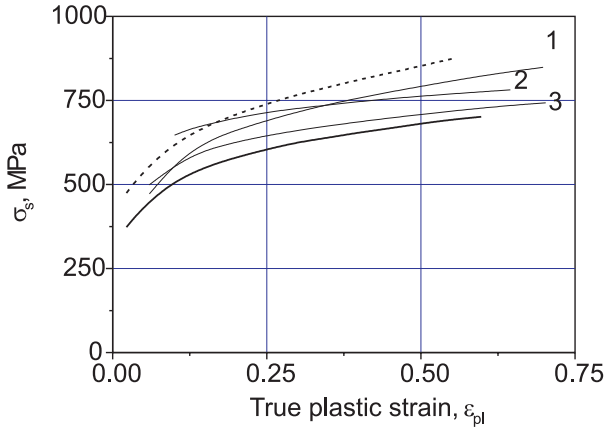

Fig. 6. Work hardening curves for steel C15 in upsetting ($t = 20\,^{\circ}$C): 1 – isothermal upsetting, $\dot{\varepsilon} = 0.25\ \mathrm{s}^{-1}$ [13]; 2 – normalised, $\dot{\varepsilon} = 1.6\ \mathrm{s}^{-1}$ [11]; 3 – $\dot{\varepsilon} = 0.25\ \mathrm{s}^{-1}$ [13]; ; thick lines: solid ($m = 770$, $n = 0.176$) dash ($m = 975$, $n = 0.198$) – variation boundaries

properties variation due to all mentioned factors (difference in chemical composition, grains structure and thermo-mechanical history). *These characteristics are used to represent properties of steel C15 and their natural variation in the Finite Element model.*

2.3. Characterisation of Fibreglass/Epoxy composite

Glass reinforced plastics have been used for years in structural engineering, although in comparatively small quantities. One of the most common constituent materials used were 'E' glass fibres, as reinforcement and epoxy resins as the matrix. These materials have been chosen, rather than others available, because they possess economic and structural properties well suited for use in the construction industry. More over, application of only glass fibre based polymer composites is possible in High Voltage power applications where good insulation properties of glass fibre composites are highly appreciated. Polymer composites are often fabricated in the form of unidirectional long fibre systems. If such composites are pultruded they have uniform cross-section along the length. Continuos fibreglass epoxy rods have a round cross section and longitudinal fibre orientation.

2.3.1. Experimental Transversal Compression

Transversal compression was performed on the MTS testing machine. Brick shaped specimens had 10 × 10 mm cross-section and 20 mm length in direction of fibres alignment. Compression was realised between rigid plane plates. Load/displacement diagram reduced to stress/strain dimensions is depicted in *Fig. 7*. Strain was assumed to be small and change in the cross-section in compression direction insignificant. Initial non-linearity is explained by contact conditions, redistribution of applied load and other factors. It may be easily eliminated by plotting a tangent (exactly, linear fitting) passing through the central part of the graph. Transversal elasticity modulus and strength are defined from each of 5 curves. Means and standard deviations are compiled in *Table 1*. Relative deviation does not exceed 4.0%. Curves demonstrate good gathering and yield the values of Young modulus and maximum compression transversal stress with relatively small scattering. *Therefore, variation of elastic constants of composite material is neglected later.*

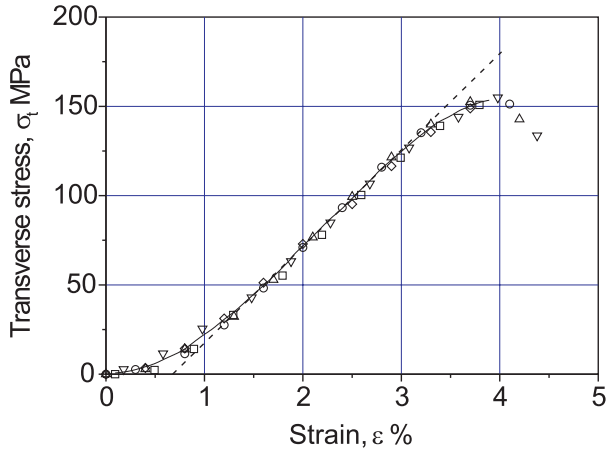

Fig. 7. Transversal compression test results: solid line, averaged by 5 test results; dash line, linear regression through the mid region

Table 1. Compilation of transverse compression test results

	Mean	Standard deviation	Relative deviation
Modulus, GPa	5.26	±0.21	±0.040
Strength, MPa	153.8	±2.2	±0.014

3. General Model of the Joint in the Cross-section

Compression scheme with radial motion of dies mentioned earlier provides uniform loading conditions at each contact surface along entire forming. This allows creation of equal degree of core's squeezing for generally varying sleeve diameter and clearance. Here mechanical model corresponding to described loading scheme in mid cross-section of the joint is introduced (*Fig. 8*). If boundary conditions constraining sides of the segments from tangential motion are fulfilled and vertex angle g satisfies relation

$$\gamma = \pi / n \tag{8}$$

for some natural number n, then stress and strain field of the entire model may be reproduced by mirroring the segment relative to corresponding segment sides. Later we consider the case $n = 8$; $\gamma = 22.5°$.

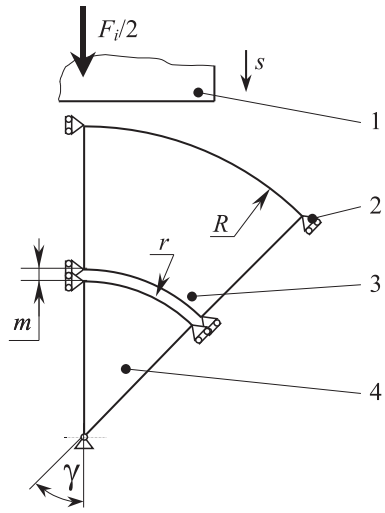

Fig. 8. General model of forming with dies of radial motion: 1 – die; 2 – tangential movement constrains; 3 – sleeve; 4 – core

Profile of the die's working face my be concave or convex and is, generally speaking, curved surface of specified configuration. Die is loaded with effective force F_i along the path s. Dies loads are equal for each surface during the entire forming process. As this study deals with 2D model actual dimensions are reduced by the axial length. Each physical value called 'normalised' or 'specific' regards unit length value. Further, reference to this model is assumed by default.

3.1. Development of the Finite Element Model

General-purpose non-linear Finite Element code Marc K7.3 has been used for the plane-strain finite element simulation in mid cross-section of the joint. Advanced FE tools such as automatic mesh generation, iterative step loading, automatic contact control and others were involved during the modelling. Details concerning particular implementation of the FE method can be found in [8].

Results of transverse compression test performed previously agreed with generally accepted opinion of small deformations to failure of reinforced polymer composites. This, combined with hydrostatic-like stress state in the composite core subjected to radial shrinkage essentially governs brittle type behaviour of the core. It means that the core's mechanical response may be represented well by linear anisotropic (more precisely: orthotropic) materials model. To formulate mechanical problem numerically a number of assumption was accepted:

- composite core is homogenous on the macro scale due to big amount of fibres randomly distributed in the matrix;
- composite core is orthotropic, elastic and obeys the Hook's law;
- steel material is homogeneous, isotropic and demonstrates elastic-plastic behaviour governed by isotropic hardening rule;
- automatic contact algorithm is used which handles contact interaction between the bodies, forming tool and symmetry plane are implicitly considered to be rigid;
- due to small relative displacement in the joint's interface and between tool and sleeve, and its little contribution to the general stiffness, friction is neglected;
- updated Lagrange procedure is employed in conjunction with finite plasticity option for elastic- plastic sleeve, which involves constitutive equations in the true stress – logarithmic strain framework, this allows to realistically handle large strains.

E-glass/Epoxy composite rod has a glass volume fraction V_f of about 60%. Since recently fibreglass/epoxy composites were intensively used, quite a big number of researchers presented analytical and experimental data on properties of this material. These data could be found in a number of works [1], [12] and others. Constants accepted for numerical calculation based on *Table 2* are given in the last row.

Table 2. Material constants of unidirectional E-glass/epoxy composites

V_f	E_1	E_2	ν_{12}	ν_{13}	G_{12}	Source
0.62	46	17	0.27	0.26	–	[1] (analyt.)
0.62	38.9	10	0.29	–	3.8	[1] (exper.)
0.60	45.6	16.2	0.278	0.4	5.83	[12]
060	40	10	0.29	0.26	4.5	Accepted

Yield criterion of elastic-plastic material is represented by von Mises yield condition. Work hardening curves for a metal component are assigned from *Fig. 6* as functions of plastic strain. Flow rule is represented by the Prandtl-Reuss relation.

Imperfect interface between rod and sleeve is analysed, so that relative sliding is allowed. It means that all parts are treated as separate entities, which exhibit discontinuous stresses and displacements across the interface, and at respective loads are capable of undergoing relative sliding.

3.1.1. FE mesh construction

A number of consequent mesh refinements were necessary to achieve satisfactory contact conditions resulting in smooth load and displacement distribution. Finally accepted FE mesh is depicted in *Fig. 9.* It accounts total of 535 nodes and 571 elements including 355 4-node and 216 3-node isoparametric plane- strain elements. The size of the smallest element in fragment (a) of *Fig. 10* is about 0.1 mm. Such fine mesh is necessary to achieve smooth load and displacement response of the tool involved in gradually extending contact with the sleeve. Expansion of the mesh in off-plane direction *z* by 300 mm avoiding exceeding element distortion (let say with the step 0.5 mm) would give 342600 8- and 6-node 3-D elements. Such model size needs substantial hardware and time resources. Not even saying that model verification and any kind of parametric study requiring multiple runs would be extremely time consuming. Finally 2-D plane-strain model was accepted for qualitative characterisation of the crimping process of tight cylindrical joint.

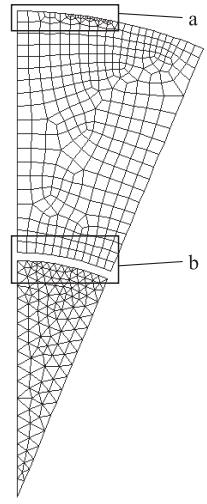

Fig. 9. Finally accepted FE mesh

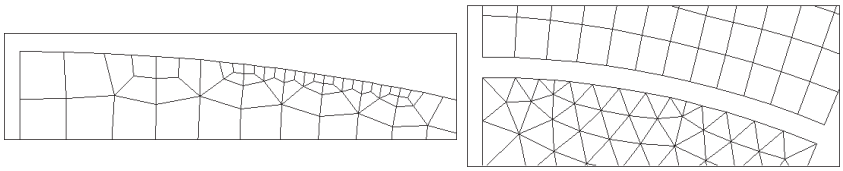

Fig. 10. Critical mesh domains (a) and (b) (zoomed)

3.1.2. Numerical integration of the strain energy

In order to provide volume integration of strain energy density subroutines in Fortran were written. Numerical integration of the strain energy density was approximately performed across the volume of each contacting body according to the following computational scheme:

$$U = \sum_{i=1}^{N} s_i h_i \overline{w}_i, \tag{9}$$

where

N	number of elements comprising given body;
$s_i = \frac{1}{2}\sum_{j=1} K_i \left(x_n - x_j\right)\left(y_n + y_j\right)$	area of the i-th element, where
K_i	number of nodes of the i-th element;
x_j, y_j	co-ordinates of the j-th node of the element;
$n = \begin{cases} j+1 & n < k, \\ 1 & n = k, \end{cases}$	for counter clock wise node numbering scheme;
h_i	is the thickness of the element;
$\overline{w}_i = \frac{1}{L_i}\sum_{j=1} L_i w_j$	average strain energy density for the element, where
L_i	number of the integration points;
w_j	strain energy density at the j-th integration point.

If thickness of the elements remains constant $h_i = h$ *Eq.* (9) can be rewritten:

$$U = h \sum_{i=1}^{N} \frac{\sum\limits_{j=1}^{K_i} \left(x_n - x_j\right)\left(y_n + y_j\right) \sum\limits_{j=1}^{L_i} w_i}{2L_i}. \tag{10}$$

4. Numerical Analysis of the System Behaviour

Load stepping involved incremental displacement-type loading divided to 30–50 increments. Each loading increment provided tool's radial motion of $12.5 \cdot 10^{-3}$ mm. As deformation proceeds resistance of the mechanical system grows. Load-displacement diagrams along the numerical simulation are depicted in *Fig. 11*. That is monotonously growing curve generally representing non-linear response of load with displacement. In the course of forming initially non-zero clearance in the interface gradually disappears. Different stages of the forming are designated as s1, s2 and s3. Three stages of the forming at different loading state correspond to certain clearance in the interface (*Fig. 12*).

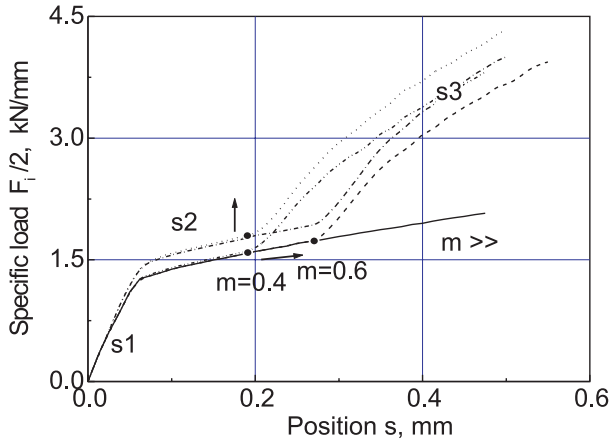

Fig. 11. Load/displacement diagrams crimping with varied dimensions and properties: solid line, empty sleeve; dash and double dot-dash lines, lower mechanical characteristic; dot and dot-dash lines, upper characteristic

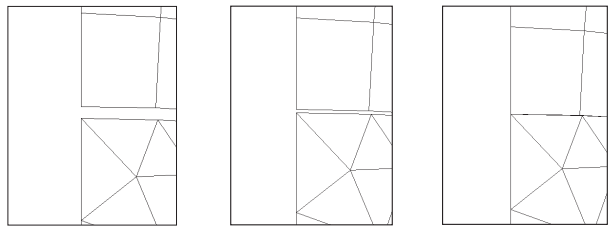

Fig. 12. Gradual clearance closure in the interface: s1 (left), s2 (middle) and s3 (right)

4.1. Analysis of the Forming Stages

Stage (s1) represents the region of the initial contact between die and sleeve. Required forming force needed to deform sleeve increases linearly in response to the stiffness of the system. Stage (s2) is characterised by development of bulk plastic deformations. Structure produces non-linear response associated with the beginning of the work hardening of the material. Significant deformations may develop during this stage. Gap between fitting and core consequently decreases. At the beginning of stage (s3) gap between core and sleeve disappears. Change in structural behaviour associated with the change in boundary conditions happens. Further radial deformations of the sleeve's inner surface are partly constrained. The forming process may be characterised as backward extrusion rather than forward extrusion. Response produced by structure is now a contribution of both fitting's and rod's stiffness. Visible stiffness increase is expected. Contact pressure develops in the interface, and rod accumulates elastic energy.

4.2. Analysis of External Work Performed on the System

Let us consider loading of static mechanical system defined above at slow rate and as succession of states of equilibrium. Then the process may be described by a scalar monotonously growing parameter representing position of one of the forming tools $s = s(t)$ in a way that $s = s_0$ corresponds to the beginning of the loading and $s = s_1$ to the end. If external equivalent load applied by the rigid tool is known, let it be $F(s)$, then mechanical work of the external forces may be written

$$W = \int_{s_0}^{s_1} F \mathrm{d}s. \tag{11}$$

Assuming that for given mechanical system external force is known both for deformation of empty sleeve (or joint with large or infinite clearance) $F_{empt}(s)$ and filled (joint with moderate clearance) $F_{fil}(s)$ we have mechanical work

$$W_{empt} = \int_{s_0}^{s_1} F_{empt} \mathrm{d}s, \tag{12}$$

and

$$W_{fil} = \int_{s_0}^{s_1} F_{fil} \mathrm{d}s, \tag{13}$$

of respective forming process till displacement s_1. Let introduce extra mechanical work W_{extra}

$$W_{extra} = W_{fil} - W_{empt} \Rightarrow \int_{s_0}^{s_1} F_{fil}\,\mathrm{d}s - \int_{s_0}^{s_1} F_{empt}\,\mathrm{d}s \overset{!}{=} \int_{s_0}^{s_1} \left(F_{fil} - F_{empt}\right)\mathrm{d}s \quad (14)$$

being complimentary mechanical work needed to deform filled sleeve in the interval (s_0, s_1) compare to the deformation work of equivalent empty sleeve. Extra mechanical work is simply illustrated graphically (*Fig 13*). That is the area encapsulated between load/displacement diagrams $F_{fil}(s)$ and $F_{empt}(s)$ in the interval (s_0, s_1).

Let say some words about deformation process, and elastic energy of the core. Such displacement s_k exists ($s_k \leq s_1$) at which deformable bodies come in contact. Then for a loading state at $s = s_i$ strain energy of the core is zero until contact and positive later:

$$U_i^c = \begin{cases} 0, & s_i \leq s_k, \\ > 0, & s_i > s_k. \end{cases} \quad (15)$$

For given loading from s_0 to s_1 let virtually vary s_k. In the extreme case for $s_k = s_1$ energy $U_1^c = 0$. If contact will happen earlier strain energy of the core is expected to grow due to monotonous nature of loading process. As soon as sleeve comes in contact with core supplied external mechanical work goes partly on increase of the core's strain energy. One of the characteristic features of the extra work is that it starts to grow from zero only after contact in the interface independently on initial clearance and material properties or just like elastic strain energy of the core. Later it will be shown that both elastic energy of the core U_i^c and extra mechanical work W_i^{extra} (corresponding to the forming stage s_i) increase monotonously. Also, that there is one-to-one correspondence between these values. We are intended to prove as well that extra mechanical work may be used as a parameter describing strain energy and hence compression state of the core.

Well distinguished from the diagrams contact point suggests that we could try to extract information characterising behaviour of the rod. Since based on experimental knowledge behaviour of the empty fitting may be further extrapolated to the large deformations range mechanical work W_{extra} may be estimated even online. Until certain limit composite rod would be deformed as an elastic body, thus neglecting inelastic energy dissipation mechanical work performed on composite rod transforms partly to the elastic energy.

4.3. Illustration of Proposed Method

Proposed control model may be illustrated with the help of the piece-wise linear model. Here (*Fig. 13*), outlined triangles represent an area between respective load diagrams of filled and empty sleeve being extra mechanical work W_{extra}. With the

help of *Fig. 3* it may be seen that variation of lower vertex and both associated with it slopes is possible due to change in dimensions and mechanical properties of metal sleeve. Assuming that top vertex of each triangle in load-position space corresponds to equal degree of core's compression, we say that areas of triangles are equal. End criteria presented as F_c and s_c is valid for only one of them.

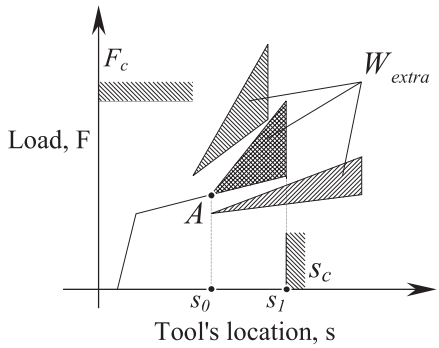

Fig. 13. Piece-wise linear model of the of the crimping in the load-position space

One of the most striking advantages of the method well depicted here is that independently to the location of triangle in the absolute co-ordinate system, compression state of the core is mainly reflected by the triangle's area (or extra mechanical work W_{extra}).

4.4. Analysis of the Core's Strain Energy Transformation

Strain energy of the core was integrated numerically according to *Eq.* (10). Given, initial gap is non zero, any external work can be only performed on the core just after physical contact between core and fitting had happened, in other words the clearance had been partly or completely filled. Thus contact in the interface may be detected by inclination of the core's strain energy from the zero level. Comparison of load/displacement curves of filled and empty sleeves squeezing with respective core's energy suggests that contact point may be identified from the inclination of the mechanical characteristic as well. Loading diagrams of medium fits (clearance 0.4 mm) were presented in *Fig. 11*. Increase of the initial clearance to 0.6 mm shifts curves to the right. Solid curve represents behaviour of the empty fitting obtained by squeezing of the sleeve of identical material and dimensions.

Plotting extra work of tight and loose joint versus strain energy (*Fig. 14*) demonstrates fairly good prediction of compression state of the core by introduced parameter. It is essentially invariant to magnitude of initial clearance and squeezing load and hence should be able of reliable performance in varying production environment.

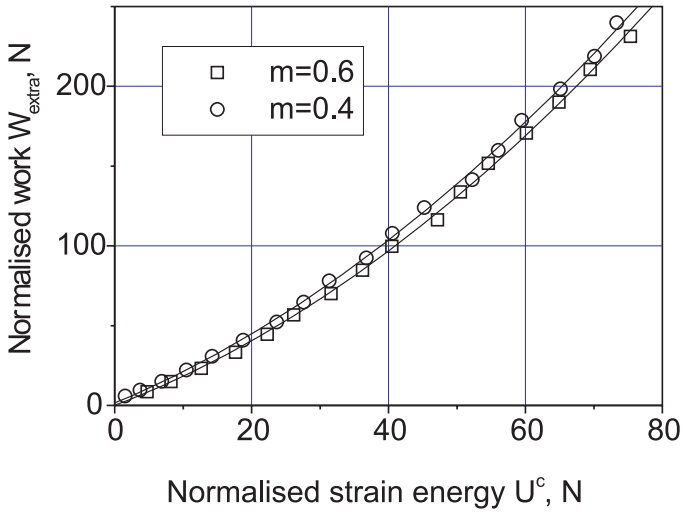

Fig. 14. Relation of strain energy and extra work for $m = 0.6$ mm and $m = 0.4$ mm clearance

4.5. Parametric Study with the FE Model

Residual strain energy of the core is considered to realistically represent residual compression state of the core and, hence, load-bearing capacity of the joint. It is found by simulation of full loading-unloading cycle. The value of strain energy at completely released load is called residual strain energy U^c_{res}. Load F, position s and extra work W_{extra} are compared in respect to provide better functional relation with the energy. Material properties of the fitting are simulated for 'upper' and 'lower' curves (*Fig. 6*), dimensions by two values of clearance 0.4 and 0.6.

Each point on scatters in *Fig. 15* represents results of one simulation till certain compression state. Correlation coefficient R provides the measure of linear relation between variables. Polynomial trendlines in *Fig. 15* (right) help to identify influence of dimensions and materials properties on each of the parameters. Possible control error (or energy scattering) is illustrated by U_{err}. It is the smallest for control by certain value of extra work. Simulation predicts approximately $\pm 25\%$ scattering for control by position. Error of extra work method is about 4 times smaller.

Effect of dimensions and material properties is the most characteristic while controlling for position. Clearance increase simply shifts the trendline upwards, while alteration of properties affects the tangent. For control by position the most disadvantageous combination is given by 'lower-0.6' and 'upper-0.4'. While for both load control and extra work control by 'lower-0.4' and 'upper-0.6'.

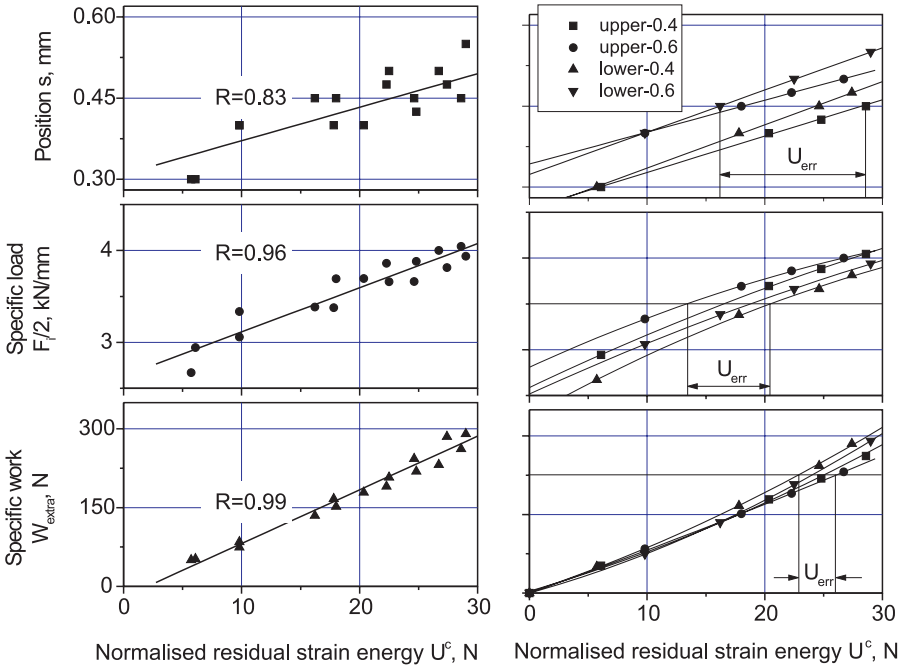

Fig. 15. FE calculated control parameters versus residual strain energy of the core

5. Conclusions

1. Two factors mainly affecting assembling process and resulting joint performance were identified. They are scattering of dimensions and mechanical properties. Restriction of the chemical composition termo-mechanical treatment of steel and surface finishing expected to essentially rise the cost, while the main problem would remain unaffected. Possible scattering of initial clearance in the interface, mechanical characteristics of some carbon steels and compression properties of fibreglass epoxy composites was conducted in details:
   - Analysis of accepted tolerance on parts diameters in the interface allowed defining clearance variation. Value of 0.2 mm is accepted for parametric FE study.
   - Upsetting carbon steel MSZT Fe235B specimens demonstrated large scattering of mechanical properties. Lower and upper boundaries of mechanical characteristics provided for FE study were assigned based on the literature data on carbon steel C15.
   - Variation of elastic constants of fibreglass epoxy proved to be small (below 4%) and was excluded from the consideration.
2. Finite element model including formulation of boundary conditions, selection

of the mesh refinement, assignment of particular dimensions and materials low with respective upper and lower variation boundaries was performed enabling qualitative evaluation of components stress-strain state, applied load and working displacement during the crimping.
Residual elastic strain energy of composite core was chosen as an integral measure of the joint compression degree and, hence, resulting load-bearing capacity. Subroutines in Fortran run with the commercial FE were developed enabling numerical integration of the strain energy density at the deformed bodies across the cross-section.
Qualitative differences were observed between load diagrams of empty sleeve and medium fit. Gap closure detected from the FE model coincided with inflexion on the load diagram. This enabled exact determination of contact point from the compression diagram.

3. Parametric study was performed by consequent run of the FE model with different values of varied parameters and maximum load/position. Each run of the model resulted in 4 discrete values of maximum load, maximum position, extra work and residual strain energy of the composite core.
   - Results of evaluation revealed the highest correlation of strain energy with extra mechanical work.
   - Possible energy error if controlling by extra work was fount to be 4 times smaller as compared with control by position and 2 times smaller as compared with control by load.
   - Effect of dimensions and material properties was wound to be most characteristic while controlling for position. Clearance increase simply shifts the trendline, while alteration of properties affects the angle.
   - Scattering of mechanical characteristics of the steel sleeve resulted in variation of the core compression degree while crimping for the same forming load. Stiffer characteristics corresponded to lower residual strain energy of the cores.

Extra mechanical work parameter was finally found to behave in the most similar manner to the calculated strain energy of the core. It appeared to be a function of the core's strain energy most robust to the variation of dimensions and load.

Acknowledgement

Warmest thanks are expressed to the stuff of the Department of Materials Science and Engineering. Authors would like to thank Mr. Márton Téglás (Furukawa Composite Insulators Ltd.) for co-working, his contribution and valuable advises. Our sincere appreciation goes to the Furukawa Electric Institute of Technology and The Furukawa Electric Co. for the financial support.

References

[1] BANSAL, A. – SCHUBERT, A. – BALAKRISHMAN, M. V. - KUMOSA, M. (1995): Finite Element Analysis of Substation Composite Insulators. *Composite science and technology,* Vol. 55, pp. 375–389.

[2] BENEVOLENSKI, O. I. – KRÁLLICS, GY. – KLEKOVKIN, V. S. (1997): Implementation of the Push-out Test for Improving of Composite Insulator end-Fitting Performance, *Periodica Polytechnica Ser. Mech. Eng.,* Vol. 41, No. 1, pp. 55–67.

[3] BENEVOLENSKI, O. I. (1999): Development of a Control Method in Crimping of Cylindrical Joints Comprising Polymer Composite Cores, Ph.D. Thesis, TU Budapest.

[4] BENEVOLENSKI, O. – TÉGLÁS, M. (1998): Eljárás és berendezés műanyag kompozit rúdból, és hozzá illesztett fém végdarabból álló kötés előállítására, valamint illesztett végdarabbal ellátott kompozit szigetelő. *Patent Application to the Hungarian Patent Office,* (in Hungarian), priority number P9802591, submitted.

[5] CHERNEY, E. A. (1995): Important Aspects of Non-ceramic Insulator Design. Proceedings of Symposium on Non-Ceramic Insulator Technology, Zurich, Switzerland, November 16–17.

[6] ISHIBARA, T. – KOJIRUA, M. (1987): Electrical Insulator Including Metal Sleeve Compressed Onto a Fiber Reinforced Plastic Rod and Method of Assembling the Same. US Patent No. 4,654,478.

[7] JUVINALL, R. C. – MARSHEK, K. M. (1991): Fundamentals of Machine Component Design, 2nd edition, John Willey & Sons.

[8] (1997): MARC Volume A: Theory and User Information, Version K7, MARC Analysis Research Corporation, USA.

[9] PLEHN, H. J. (1973): Berg und Huttenmannische Monatshefte, Wien, 3, S. 48–60.

[10] PYSZ, G. (1998): Zum einfluss des Spannungszustands auf die Kenngrössen des Zugversuchs. Zusammenhang zwischen Spannung und Formänderung. *Neue Hütte,* Vol. II, no. 10, S. 611–615.

[11] SCHWANDT, S. (1970): Das Formänderungsverhalten unlegiegter und niedrilegierter Stähle bei der Massivumformung. Draht, *Welt,* Vol. 56, No. 10, S. 574–581.

[12] SODEN, P. D. – HINTON, M. G. – KADDOUR, A. S. (1998): Lamina Properties, Lay-up Configurations and Loading Conditions for a Range Fibre Reinforced Composite Laminates. *Composites Science and Technology,* Vol. 58, (7), pp. 1011.

[13] KROHA V. A. (1980): Uprochnenenie metallov pri holodnij plasticheskoj deformacii, Sprabochnik, Moskva, Masinostroenie.

[14] LAHTIN, JU. M. (1983): Metallovedenie termicheskaja obrabotka metallov, Izdanie 3nd , Moskva, Metallurgia.